Hydrogel Containing Nanoparticle-Stabilized Liposomes for Topical Antimicrobial Delivery

Weiwei Gao,[†,‡] Drew Vecchio,[†] Jieming Li,[†] Jingying Zhu,[†,§] Qiangzhe Zhang,[†,‡] Victoria Fu,[†,‡] Jiayang Li,[†] Soracha Thamphiwatana,[†,‡] Diannan Lu,[§] and Liangfang Zhang[†,‡,*]

[†]Department of NanoEngineering, [‡]Moores Cancer Center, University of California, San Diego, La Jolla, California 92093, United States, and [§]Department of Chemical Engineering, Tsinghua University, Beijing 100084, China

ABSTRACT Adsorbing small charged nanoparticles onto the outer surfaces of liposomes has become an effective strategy to stabilize liposomes against fusion prior to "seeing" target bacteria, yet allow them to fuse with the bacteria upon arrival at the infection sites. As a result, nanoparticle-stabilized liposomes have become an emerging drug delivery platform for treatment of various bacterial infections. To facilitate the translation of this platform for clinical tests and uses, herein we integrate nanoparticle-stabilized liposomes with hydrogel technology for more effective and sustained topical drug delivery. The hydrogel formulation not only preserves the structural integrity of the nanoparticle-stabilized liposomes, but also allows for controllable viscoelasticity and tunable liposome release rate. Using *Staphylococcus aureus* bacteria as a model pathogen, we demonstrate that the hydrogel formulation can effectively release nanoparticle-stabilized liposomes to

Nanoparticle-stabilized liposome / Hydrogel

the bacterial culture, which subsequently fuse with bacterial membrane in a pH-dependent manner. When topically applied onto mouse skin, the hydrogel formulation does not generate any observable skin toxicity within a 7-day treatment. Collectively, the hydrogel containing nanoparticle-stabilized liposomes hold great promise for topical applications against various microbial infections.
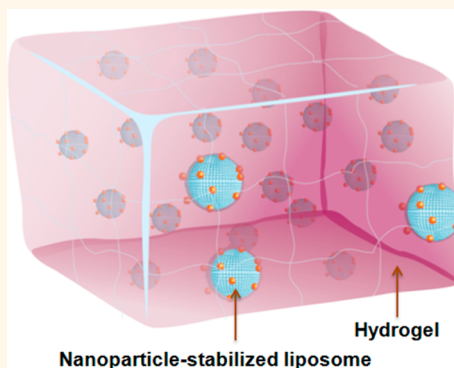
KEYWORDS: hydrogel · liposome · gold nanoparticle · vesicle fusion · antimicrobial delivery

Liposomes have attracted significant attention as a class of antimicrobial delivery vehicles owing to their unique features including biocompatible lipid materials, a bilayer structure capable of fusing with microbial membrane, readily modifiable formulation properties, and high drug loading capacity.[1−3] However, the applications of liposomes, particularly those with sizes below 100 nm, are often hindered by their poor stability due to spontaneous fusion among liposomes, causing payload loss and undesired mixing.[4,5] Using polymers such as poly(ethylene glycol) (PEG) to coat liposome surface is a common strategy to stabilize liposomes.[6,7] The PEG coating prevents liposomes from aggregation and fusion by providing steric hindrance; it also suppresses nonspecific interactions of liposomes with blood components (opsonization) and thus significantly improves liposome blood residency time.[8,9] Despite these advantages, PEGylated liposomes are less frequently used

for topical applications to treat bacterial infections. This is mainly because the polymer coating not only stabilizes liposomes against fusion with each other but also prevents them from fusing with bacterial membranes, to which the antimicrobial payloads need to be delivered.[10,11] Therefore, liposome formulations that are stabilized against fusion prior to "seeing" target bacteria, yet can resume their fusion activity once reaching the infection sites are highly desirable.

To address this challenge, an emerging strategy to stabilize liposomes for effective antimicrobial delivery, especially for topical administrations, is to adsorb small charged nanoparticles onto liposome surfaces.[12−14] The nonspecific adsorption of charged nanoparticles onto phospholipid bilayers provides steric repulsion that inhibits liposome fusion. It can also reduce liposome surface tension and further enhance liposome stability.[15,16] Intriguingly, the charge and charge density of both the nanoparticle stabilizers and the
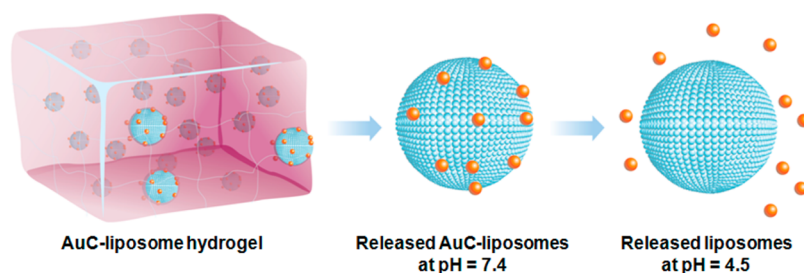
Figure 1. Schematic illustration of hydrogel containing nanoparticle-stabilized liposomes for topical antimicrobial delivery. Carboxyl-modified gold nanoparticles (AuC) were adsorbed onto the outer surfaces of cationic liposomes to stabilize them against fusion. The AuC−liposomes were subsequently embedded into an acrylamide-based hydrogel. At physiological pH (pH = 7.4), AuC−liposomes were released from the hydrogel in their entirety. When the pH drops below the pK_a value of the carboxylic group ($pK_a \sim 5$), the AuC stabilizers detached from the liposomes, resulting in the formation of bare liposomes with resumed fusion activity.

liposomes can be precisely tailored to enable stimulus-responsive binding and detaching of the nanoparticles, thereby allowing for an on-demand control over liposome fusion activity for smart drug delivery. For instance, cationic liposomes bound with negatively charged gold nanoparticles only fuse with bacteria at acidic pH, and are therefore suitable to treat various skin pathogens that thrive in acidic infection sites such as *Propionibacterium acnes*.[17] Conversely, anionic liposomes stabilized by positively charged gold nanoparticles are highly stable in gastric acid, but capable of fusing with bacteria at physiological pH, making them suitable to treat gastric pathogens such as *Helicobacter pylori*.[18] Even in the absence of such stimulus-responsive binding and detaching of the nanoparticle stabilizers, these stabilized liposomes still preserve a substantial fraction of their surface areas untouched and highly accessible to bacterial toxins. This feature allows the liposomes to respond to various bacteria such as *Staphylococcus aureus* (*S. aureus*) that secrete pore-forming toxins to trigger drug release from the liposomes.[19]

With the rapid development of nanoparticle-stabilized liposomes as an emerging antimicrobial delivery platform underlined by the various exciting stimulus-responsive drug release mechanisms, a practical and reliable formulation of such nanodelivery platform is urgently needed for enabling preclinical and clinical tests. To address this unmet need, using hydrogels as a vehicle to incorporate nanoparticle-stabilized liposomes for topical applications represents a promising solution.[20,21] Hydrogels are hydrophilic 3D polymer networks with established applications in tissue engineering and drug delivery.[22−24] Hydrogels with high water content, tunable viscoelasticity, and biocompatibility, have been intensively explored to enable topical delivery of bioactive molecules, with some successes in delivering conventional liposomes.[25,26] More importantly, successful integration of nanoparticle-stabilized liposomes with polymeric hydrogels will combine the advantages of the two distinct drug delivery platforms and thus open

the door to more advanced topical drug delivery with unique benefits such as improved tissue localization, minimized burst release, and controlled sequential drug release.[27−31]

Herein, we report the development of a hydrogel formulation that contains pH-responsive gold nanoparticle-stabilized liposomes suitable for topical antimicrobial delivery (Figure 1). In this study, carboxyl-modified gold nanoparticles (AuC) were used as stabilizers for cationic liposomes (denoted AuC−liposomes). We chose a chemically cross-linked polyacrylamide gel as a model hydrogel system for its simple preparation, high stability, and intensive clinical uses.[32,33] We showed that the hydrogel viscoelasticity could be precisely tailored by varying the cross-linker concentration, which subsequently resulted in tunable release kinetics of the incorporated AuC−liposomes. We further demonstrated that the hydrogel formulation preserved the structural integrity of the nanoparticle-stabilized liposomes and the released liposomes could fuse with bacterial membranes in response to acidic environment (*i.e.*, pH = 4.5) relevant to various skin infections.[34−37] In addition, when topically applied on mouse skin, the AuC−liposome hydrogel formulation did not generate any observable skin reaction and toxicity within a 7-day treatment, implying its potential as a safe and effective topical treatment option against skin microbial infections.

RESULTS AND DISCUSSION

The preparation of AuC−liposome hydrogel can be divided into two steps. In the first step, we prepared AuC−liposomes by following a previously established protocol.[17] Briefly, cationic phospholipid liposomes consisting of 90 wt % hydrogenated L-α-phosphatidyl-choline (EggPC) and 10 wt % 1,2-di-(9Z-octadecenoyl)-3-trimethylammonium propane (DOTAP) were prepared through the standard extrusion method, followed by mixing with AuC at a liposome-to-AuC molar ratio of 1:200. Consistent with our previous finding, this ratio ensured that the amount of AuC adsorbed onto the liposome surface effectively prevented liposome fusion
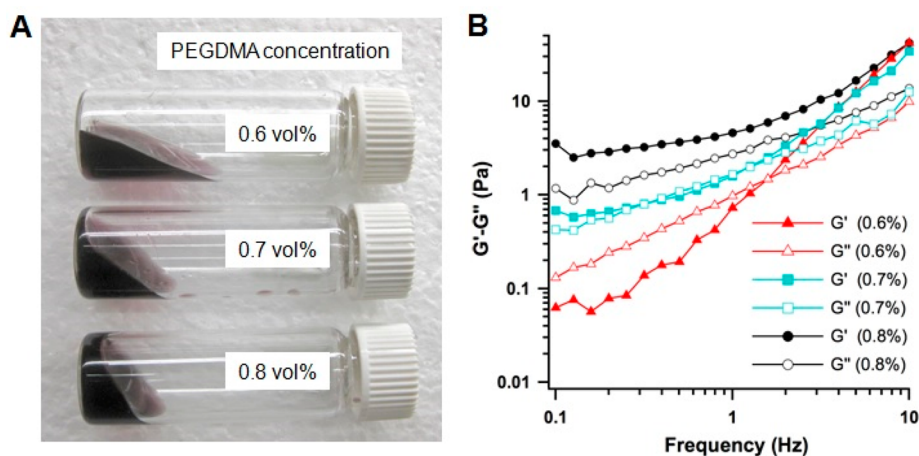
Figure 2. Formulation and rheological characterizations of AuC−liposome hydrogels. (A) A photograph of hydrogel samples made with three different cross-linker concentrations of 0.6, 0.7, and 0.8 vol %, respectively. (B) The storage modulus G' and loss modulus G'' were plotted logarithmically against frequency (0.1−10 Hz at 25 °C) of the corresponding hydrogel samples.

in suspensions.[17] In the second step, we prepared AuC−liposome hydrogel by mixing AuC−liposomes with acrylamide as the monomer and poly(ethylene glycol) dimethacrylate (PEGDMA) as the cross-linker. Hydrogelation was initiated by adding ammonium persulfate and tetramethylethylenediamine (TEMED). The reaction was allowed to proceed for 12 h at room temperature. In the following studies, we kept the concentrations of AuC−liposome, acrylamide, ammonium persulfate, and TEMED constant at 1 mg/mL (lipid content), 40 mg/mL, 1 mg/mL and 1 μL/mL, respectively, and explored three different PEGDMA concentrations of 0.6, 0.7, and 0.8 vol % to study the corresponding hydrogel rheological properties and liposome release profiles.

The hydrogelation process was allowed to proceed at room temperature for 4 h. Following the reaction, the cherry red color characteristic to the AuC nanoparticles due to their surface plasmon resonance was preserved in all samples. Morphological observation of the hydrogel showed that both AuC nanoparticles and the liposomes were uniformly distributed in the gel (Figure S1). Comparison of the AuC nanoparticle surface plasmon resonance absorption indicated the absence of gold aggregation during gel formation and 7-day storage at 4 °C (Figure S2). Apparently, increasing the cross-linker concentration resulted in hydrogels with increasing viscosity (Figure 2A). When the cross-linker concentrations were kept at 0.6 or 0.7 vol %, the resulting hydrogels behaved as viscous solutions that flew readily in the tilted vial with the latter more viscous. In contrast, when the cross-linker concentration was increased to 0.8 vol %, a freestanding hydrogel was formed. The visible viscosity differences were further quantified by dynamic rheological measurements of the storage modulus (G') and the loss modulus (G'') as a function of frequency (Figure 2B). Samples with 0.6 vol % of cross-linker concentration

showed the $G'-G''$ crossover and a strong dependency of both moduli on frequency, suggesting that the hydrogel behaved as an entanglement network and the sample was primarily viscous rather than elastic. At 0.7 vol % of the cross-linker concentration, both G' and G'' increased accordingly and their values came close at low frequencies (<1 Hz), indicating a transition from fluidic to more gel-like viscoelastic behavior. When the cross-linker concentration was further increased to 0.8 vol %, G' exceeded G'' over the entire frequency range tested in the study, suggesting the formation of a hydrogel network.

Following the preparation of AuC−liposome hydrogel, we examined the structural integrity of the AuC−liposomes incorporated in the hydrogel. To do so, we compared the size and surface zeta potential of the AuC−liposomes released from the hydrogel to those of the bare liposomes and the unincorporated AuC−liposomes at neutral pH (Figure 3). Dynamic light scattering (DLS) measurements of the bare liposomes showed a diameter of 91.2 ± 0.9 nm (polydispersity index = 0.10 ± 0.02) and a surface zeta potential of 24.9 ± 1.5 mV. The measurements of unincorporated AuC−liposomes showed a diameter of 97.1 ± 1.0 nm (polydispersity index = 0.14 ± 0.02) and a surface zeta potential of −25.3 ± 0.7 mV. The slight size increase and the switch of surface charge from a positive value to a negative one were resulted from the attachment of AuC stabilizers to the liposomes. Then the AuC−liposomes were used to make hydrogels. Following the hydrogelation, hydrogel samples were immersed in water at pH = 7.4 and 37 °C. After 30-min incubation, we were able to detect released AuC−liposomes by using DLS. In the study, the variation of PEGDMA concentrations showed no effect on the values of liposome size and zeta potential. DLS measurements on the released AuC−liposomes showed an average diameter of 97.6 ± 1.1 nm (polydispersity index = 0.16 ± 0.03)
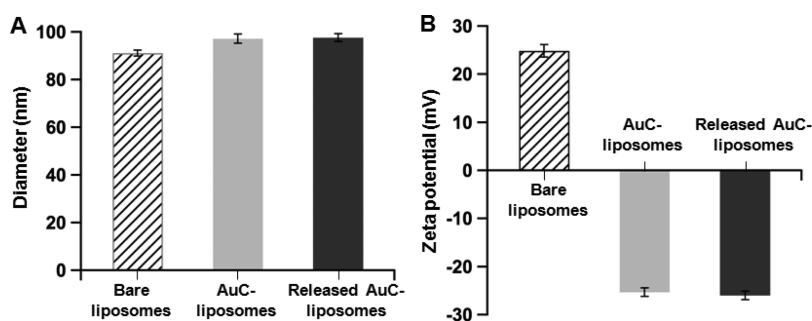
Figure 3. Hydrodynamic size (A) and surface zeta potential (B) of bare liposomes (without AuC stabilizer), AuC−liposomes prior to the hydrogel incorporation, and AuC−liposomes released from the hydrogel.
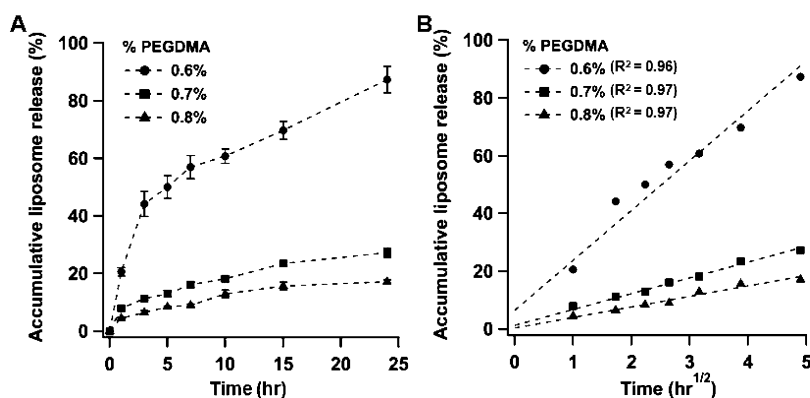

Figure 4. Hydrogel-mediated liposome release. (A) Accumulative liposome release profile from the AuC−liposome hydrogels made with three different cross-linker concentrations of 0.6, 0.7, and 0.8 vol %, respectively. (B) The corresponding liposome release percentage was plotted against the square root of release time, which yielded linear fittings using a diffusion-dominant Higuchi model.

and a surface zeta potential of −26.0 ± 1.9 mV. These values match those of the unincorporated AuC−liposomes. Further study showed that the released AuC−liposomes remained stable at pH = 7.4 when the hydrogel was incubated for up to 7 days (Figure S3). These results suggest that the hydrogel formulation developed in this study is capable of preserving the integrity of the AuC−liposomes during the incorporation.

Next, we investigated the release kinetics of AuC−liposomes from the hydrogels with different cross-linker concentrations. The amount of released liposomes was quantified by measuring the amount of liposome-bound rhodamine B (RhB) dye detected in the incubation solution. Overall, increasing the cross-linker concentration resulted in a decreased liposome release rate (Figure 4A). Specifically, for the hydrogel sample with 0.6 vol % of the cross-linker, nearly 90% liposomes were released within 24 h. When the cross-linker concentration was increased to 0.7 and 0.8 vol %, within the first 24 h, only 25% and 17% liposomes were released, respectively. To gain a quantitative understanding of how cross-linker concentration affected AuC−liposome release, the liposome release profiles were analyzed using mathematical models established in previous hydrogel-mediated drug release studies.[38,39] The use of polyacrylamide hydrogel

allows us to hypothesize that the liposome release kinetics are primarily dominated by diffusional liposome efflux with negligible contributions from the hydrogel network.[40] Therefore, a diffusion-dominant Higuchi model was applied to analyze the liposome release profiles: $M_t = Kt^{1/2}$, where M_t is drug release at time t in hours and K is the Higuchi constant.[41,42] Plotting the liposome release percentage against the square root of time yielded linear fittings with $R^2 = 0.96$, 0.97, and 0.97 for the three cross-linker concentrations of 0.6, 0.7, and 0.8 vol %, respectively (Figure 4B). The goodness of the fit indicates a diffusion-controlled liposome release mechanism. On the basis of this analysis, we determined the Higuchi constants of the three hydrogel formulations to be 17.3 ± 1.8, 5.5 ± 0.4, and 3.6 ± 0.3 h$^{-1/2}$, respectively.

Following the release study, we tested the pH-dependent fusion activity of the AuC−liposomes released from the hydrogels by using *S. aureus* bacteria. The hallmark of liposome-based antimicrobial activity is the ability of liposomes to fuse with bacteria, which either directly disrupt bacterial membrane or facilitate the release of antimicrobial agents directly into the bacterial cells.[3,18] On the basis of this property, we chose a liposome−bacterium fusion assay to study the fusion activity of the released liposomes and to evaluate the potential antibacterial activity of the
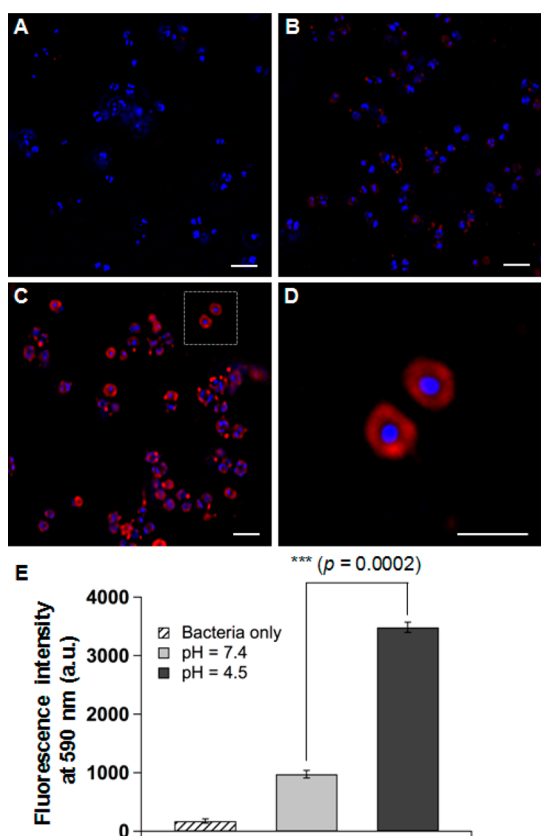
Figure 5. Fluorescence study of the fusion interaction between hydrogel-released liposomes and S. aureus bacteria. Liposomes were labeled with fluorescent dye RhB (red) and the bacteria were stained with DAPI (blue). (A) Control bacteria without any treatment, (B) bacteria incubated with AuC−liposome hydrogel (PEGDMA 0.8 vol %) at pH = 7.4, (C) bacteria incubated with AuC−liposome hydrogel (PEGDMA 0.8 vol %) at pH = 4.5, (D) a zoomed-in image of (C), and (E) overall fluorescence intensity comparison of the bacterial samples of (A−C). The scale bars in (A−D) represent 1 μm.

AuC−liposome hydrogel. In the study, S. aureus bacteria (strain MRSA252) (5×10^8 CFU in 1 mL buffer) were added to AuC−liposome hydrogel made with 0.8 vol % of PEGDMA and 0.5 mol % RhB-labeled liposomes, followed by adjusting the buffer pH to 7.4 and 4.5, respectively. The mixture suspensions were incubated at 37 °C for 30 min. Then the bacteria were thoroughly washed before observation under fluorescence microscope. For untreated bacteria, as shown in Figure 5A, only nucleoids stained with DAPI (blue) were seen. However, when the bacteria were incubated with AuC−liposome hydrogel (containing RhB-labeled liposomes) at pH = 7.4 for 30 min, sporadic red dots in the peripheral area of the bacterial nucleoid were visible (Figure 5B). Such weak fluorescence intensity is likely due to physical adsorption of AuC−liposomes onto the bacterial surface. In contrast, when the bacteria were incubated with AuC−liposome hydrogel at pH = 4.5, a significant increase of RhB fluorescence signal around the bacterial nucleoid was observed, suggesting an elevated fusion activity corresponding to the decrease of pH value (Figure 5C). In addition, the
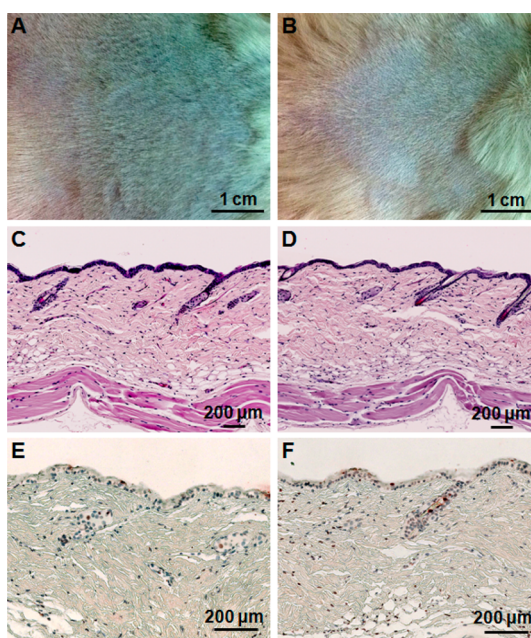

Figure 6. Toxicity evaluation of the AuC−liposome hydrogel using a mouse skin model. Mouse skin was treated with PBS buffer (A, C, and E) and AuC−liposome hydrogel (B, D, and F), respectively. Following the treatment, the skin morphology of the two treatment groups was examined (A and B). The skin sections were further examined after H&E staining (C and D) and TUNEL staining (E and F).

fluorescence image clearly reflected the spherical shape of individual bacteria and the grape-like clusters of the bacterial colony, which were characteristic of S. aureus bacteria.[43] A zoomed-in image further demonstrated the bacteria after their incubation with the hydrogel at a subcellular resolution (Figure 5D). In this image, RhB signal was exclusively and evenly distributed around the bacterial nucleoid, consistent with the fusion between liposomes and the bacterial membrane.

The microscopic observations were further confirmed by directly measuring the overall fluorescence intensity of the bacteria after their incubation with the hydrogel samples. As shown in Figure 5E, S. aureus bacteria incubated with the AuC−liposome hydrogel at pH = 4.5 showed a significantly higher level of fluorescence. In contrast, much weaker fluorescence emission was observed from the bacteria incubated with the hydrogel at pH = 7.4. Such differential liposome-bacterium fusion activity clearly demonstrates that the AuC−liposome hydrogel formulation can readily release AuC−liposomes to the bacterial culture, which then fuse with bacterial membrane in a pH-dependent fashion. This result also indicates the antimicrobial potential of the AuC−liposome hydrogel once bactericidal agents are loaded into the liposomes.

Finally, we evaluated the toxicity of the AuC−liposome hydrogel by using a mouse skin model. In this study, the mouse back skin was shaved 24 h prior to gel application to allow the skin to recover from any

possible disturbance to the stratum corneum and then moistened with PBS right before the experiments. Then the hydrogel samples were topically applied onto the skin and kept for 24 h. The back of each mouse was cleaned every day before the new administration of the hydrogel. After a 7-day treatment, mouse skin treated with AuC—liposome hydrogel maintained its normal structure without any indications of toxicity such as erythema and edema. This skin structure resembles that treated with blank PBS buffer, which served as a negative control (Figure 6A,B). Following the skin morphology examination, a skin biopsy was collected at the end of the treatment and stained with hematoxylin and eosin (H&E). The AuC—liposome hydrogel treated skin maintained an undisturbed structure with a clear layer of healthy epidermal cells on top of the dermis layer, which was identical to the PBS treated skin sample (Figure 6C,D). The hydrogel toxicity was further evaluated by using a terminal deoxynucleotidyl transferase-mediated deoxyuridine triphosphate nick-end labeling (TUNEL) assay to examine the viability of skin sections under the experimental conditions. Compared to the PBS control, there was no apparent increase of apoptotic staining in AuC—liposome hydrogel treated skin (Figure 6E,F).

The absence of any skin reaction and toxicity within a 7-day treatment suggests that topically applying AuC—liposome hydrogels is safe.

CONCLUSION

In this study, we developed a hydrogel formulation that contains pH-responsive gold nanoparticle-stabilized liposomes for topical antimicrobial delivery. The viscoeleasticity of the hydrogel was precisely tailored by varying the cross-linker concentration, which resulted in tunable release kinetics of the incorporated liposomes. We also demonstrated that the hydrogel formulation preserved the structural integrity of the nanoparticle-stabilized liposomes. Using *S. aureus* bacteria as a model pathogen, we showed that the hydrogel formulation could effectively release nanoparticle-stabilized liposomes to the bacterial culture, which subsequently fused with bacterial membrane in a pH-dependent manner. In addition, when topically applied onto mouse skin, the hydrogel formulation did not generate any skin reaction within a 7-day treatment. Taken together, integrating nanoparticle-stabilized liposomes with hydrogel technology provides a unique and robust hybrid formulation for topical drug delivery against microbial infections.

EXPERIMENTAL SECTION

Materials. Phospholipids including hydrogenated L-α-phosphatidylcholine (EggPC), 1,2-di-(9Z-octadecenoyl)-3-trimethyl-lammonium propane (DOTAP), and 1, 2-dimyristoyl-*sn*-glycero-3-phosphoethanolamine-*N*-lissamine rhodamine B sulfonyl (DMPE-RhB) were purchased from Avanti Polar Lipids, Inc. To prepare carboxyl-functionalized gold nanoparticles (AuC), the following chemicals were purchased: hydrogen tetrachloroaurate (HAuCl₄) (ACROS Organics), sodium borohydride (NaBH₄) (ACROS Organics), and 3-mercaptopropionic acid (MPA, Sigma-Aldrich). To prepare hydrogel, acrylamide (used as the monomer), poly(ethylene glycol) dimethacrylate, (PEGDMA, used as the cross-linker), tetramethylethylene diamine (TEMED) and ammonium persulfate (both used as initiators) were purchased from Sigma-Aldrich. Potassium hydrogen phthalate and potassium phosphate monobasic were purchased from EMD and Sigma Aldrich, respectively, in order to prepare buffer solutions.

Preparation of AuC. The AuC nanoparticles were prepared using a sodium borohydride reduction method following a previously published protocol.[17,44] Briefly, aqueous solution of HAuCl₄ (0.1 mM, 50 mL) was reduced by 5 mg of NaBH₄ on an ice bath, resulting in the formation of bare gold nanoparticles. Then the bare gold nanoparticles were functionalized with carboxyl groups by overnight incubation with MPA (4×10^{-4} M) at room temperature. Following the reaction, the AuC nanoparticle suspension was washed three times using an Amicon Ultra-4 centrifugal filter with a molecular weight cutoff of 10 kDa (Millipore, Billerica, MA) and then suspended in aqueous solution at pH = 7.4. Transmission electron microscope (TEM) analysis confirmed that the AuC nanoparticles had a nearly uniform size of ~4 nm in diameter and the dynamic light scattering (DLS) measurements showed a negative surface zeta potential of -24.8 ± 3.5 mV, both consistent with previous studies.[17,44]

Preparation of AuC—Liposomes. Cationic liposomes consisting of EggPC (zwitterionic phospholipid) and DOTAP (cationic

phospholipid) were prepared *via* the standard extrusion method.[45] Briefly, 1 mg of EggPC and DOTAP mixture (weight ratio = 9:1) was dissolved in 1 mL of chloroform. The solvent was evaporated by gently blowing nitrogen gas over it for 15 min. Then, the dried lipid films were hydrated with 1 mL of deionized water, followed by vortexing for 1 min and sonicating for 3 min in a bath sonicator (Fisher Scientific FS30D) to produce multi-lamellar vesicles (MLVs). A Ti probe (Branson 450 sonifier) was used to sonicate the MLVs for 1—2 min at 20 W to produce unilamellar vesicles. To form narrowly distributed small unila-mellar vesicels (SUVs), the solution was extruded through a 100 nm pore-sized polycarbonate membrane 11 times.

To prepare AuC—liposomes, the pH levels of both AuC and liposome suspensions were adjusted to 7.4 using NaOH. Then the liposomes and AuC at desired molar ratio were mixed together, followed by vortexing for 10 min. To quantify the adsorption of AuC onto the liposome surfaces, RhB-labeled liposomes were prepared by mixing 0.5 mol % of DMPE-RhB with lipid components prior to liposome preparation. The fluorescence emission spectra of RhB in the range of 550—650 nm were measured using a fluorescent spectrophotometer (Infinite M200, TECAN, Switzerland) at an excitation wavelength of 470 nm. Mixing AuC with fluorescently labeled liposomes resulted in the quenching of fluorescence intensity. Consistent with our previous studies, the quenching effect reached the maximum at an AuC-to-liposome molar ratio (M_{AuC}/M_L) of 280:1 at pH = 7.4, indicating the saturation of AuC on liposome surfaces at this molar ratio.[17] For hydrogel incorporation in this study, a smaller M_{AuC}/M_L value of 200:1 was used because this ratio was adequate for AuC to prevent liposome fusion in suspensions.

Preparation of AuC—Liposome Hydrogel. The AuC—liposome-loaded hydrogel was made by mixing AuC—liposome suspension with acrylamide, PEGDMA, ammonium persulfate, and TEMED. The final concentrations of liposomes, acrylamide, ammonium persulfate and TEMED were kept constant at 1 mg/mL, 40 mg/mL, 1 mg/mL, and 1 μL/mL, respectively, while PEGDMA concentration was tested at 6, 7, or 8 μL/mL. The liquid mixture was

vortexed for 10 min and then placed in a vacuum chamber at room temperature for 4 h to allow the complete gelation to occur.

Rheological Measurements. The rheological analysis was carried out at 25 ± 0.1 °C on a strain-controlled AR-G2 rheometer (TA Instruments Inc., New Castle, DE) with parallel-plate geometry of 22 mm in diameter. Oscillatory rheological measurements were performed in the linear viscoelastic regime. The strain was kept at 0.1% and a dynamic frequency sweep from 0.1 to 10 rad/s was conducted to measure the storage modulus G' and loss modulus G''.

Liposome Release Study. To study liposome release from the hydrogel, the AuC–liposomes were labeled with DMPE-RhB. Then 0.5 mL of hydrogel was cast in a 50 mL centrifuge tube. After the gel was fully formed (approximately 4 h), each tube was added with 50 mL DI water at pH = 7.4. The tube was then placed in an incubator at 37 °C under gentle shaking. At predetermined time points, 500 μL of liquid was collected from the tube. The hydrodynamic size and surface zeta potential of the released liposomes were measured by using the Malvern Zetasizer ZS (Malvern Instruments, U.K.). The mean diameter and zeta potential were determined through DLS and electrophoretic mobility measurements, respectively. All characterization measurements were repeated three times at 25 °C. To quantify the amount of liposomes released from the hydrogel, the pH level of the liquid taken from the tube was adjusted to pH = 4.5 by using HCl. Then 15 μL of 10% Triton X-100 was added to each tube and the microtubes were centrifuged at 14 000g for 10 min to precipitate gold nanoparticles. The fluorescence intensity of the supernatant was quantified by using a fluorescent spectrophotometer (Infinite M200, TECAN, Switzerland) at an excitation wavelength of 470 nm.

Bacterial Culture. S. aureus bacteria (strain MRSA252) were cultured on tryptic soy broth (TSB) agar overnight at 37 °C. Then a single colony was inoculated in TSB medium and the medium was cultured in a rotary shaker at 37 °C. Overnight culture was refreshed in TSB medium at 1:100 dilution and under shaking for another 3 h until the OD_{600} of the culture medium reached approximately 1.0 (logarithmic growth phase). The bacteria were then harvested by centrifugation at 5000g for 10 min, and then washed with sterile PBS twice. After the removal of PBS by centrifugation, the obtained bacteria pallet was then suspended in an appropriate amount of sterile PBS for future use.

AuC–Liposome Fusion with Bacteria. For experiments, 1 mL of S. aureus bacteria at a concentration of 5×10^8 CFU/mL (determined by OD_{600} measurement, OD_{600} = 1.0 corresponding to $\sim 1 \times 10^8$ CFU/mL) was added to 0.5 mL of hydrogel containing fluorescently labeled AuC–liposomes. The solutions were then adjusted to desired pH values. After 30 min incubation, the bacteria suspension was collected and the bacteria were washed three times. The bacterial pellets were resuspended in 1 mL of PBS (1×, 10 mM Na_2HPO_4, 2 mM KH_2PO_4, 2.7 mM KCl, and 137 mM NaCl). For microscopic study, 5 μL of bacterial suspension was dropped on a poly-L-lysine coated cover slide. After the liquid was dried at room temperature, the slide was mounted by using Vectashield mounting medium with DAPI and the fluorescence images were obtained by using a Delta Vison deconvolution microscope. To quantify the overall fluorescence intensity of the bacteria, 200 μL of bacterial suspension was added to a well of 96-plate. The fluorescence intensity was measured by using a fluorescent spectrophotometer. The experiment was carried out in triplicate and the average value was reported.

Skin Toxicity Study. To evaluate the skin toxicity of AuC–liposome hydrogel, ICR mice at 6 weeks of age were purchased from Charles River Laboratories. Mice were shaved on the back 24 h prior to the study. Then the AuC–liposome hydrogel was applied on the shaved area once daily for a period of 7 days. Mice treated with PBS served as a negative control. To prevent the gel from drying out, the skin was covered with gauzes. Twenty-four hours after the last topical administration, the mice were sacrificed and the skin was cross-sectioned by 8 mm biopsy punch for histological examination. The skin tissues from each mouse were fixed in buffered 10% formalin for 18 h and then embedded in paraffin. The tissue sections were stained with hematoxylin and eosin (H&E). Epithelial cell apoptosis was evaluated by the terminal deoxynucleotidyl transferase-mediated deoxyuridine triphosphate nick-end labeling (TUNEL) assay (Boehringer Mannheim, Indianapolis, IN). Sections were visualized by Hamamatsu Nanozommer 2.0HT. Images were processed using NDP viewer software. Five mice were used for each test group ($n = 5$).

Conflict of Interest: The authors declare no competing financial interest.

Supporting Information Available: Additional information includes the morphological observation of AuC–liposome hydrogel, and the stability of gold nanoparticles and AuC–liposomes in the hydrogel. This material is available free of charge *via* the Internet at http://pubs.acs.org.

REFERENCES AND NOTES

1. Torchilin, V. P. Recent Advances with Liposomes as Pharmaceutical Carriers. *Nat. Rev. Drug Discovery* **2005**, *4*, 145–160.
2. Zhang, L.; Pornpattananangkul, D.; Hu, C. M. J.; Huang, C. M. Development of Nanoparticles for Antimicrobial Drug Delivery. *Curr. Med. Chem.* **2010**, *17*, 585–594.
3. Gao, W.; Hu, C. M. J.; Fang, R. H.; Zhang, L. Liposome-like Nanostructures for Drug Delivery. *J. Mater. Chem. B* **2013**, *1*, 6569–6585.
4. Marrink, S. J.; Mark, A. E. The Mechanism of Vesicle Fusion as Revealed by Molecular Dynamics Simulations. *J. Am. Chem. Soc.* **2003**, *125*, 11144–11145.
5. Haluska, C. K.; Riske, K. A.; Marchi-Artzner, V.; Lehn, J.-M.; Lipowsky, R.; Dimova, R. Time Scales of Membrane Fusion Revealed by Direct Imaging of Vesicle Fusion with High Temporal Resolution. *Proc. Natl. Acad. Sci. U. S. A.* **2006**, *103*, 15841–15846.
6. Stepniewski, M.; Pasenkiewicz-Gierula, M.; Rog, T.; Danne, R.; Orlowski, A.; Karttunen, M.; Urtti, A.; Yliperttula, M.; Vuorimaa, E.; Bunker, A. Study of Pegylated Lipid Layers as a Model for Pegylated Liposome Surfaces: Molecular Dynamics Simulation and Langmuir Monolayer Studies. *Langmuir* **2011**, *27*, 7788–7798.
7. Yan, W.; Huang, L. Recent Advances in Liposome-Based Nanoparticles for Antigen Delivery. *Polym. Rev.* **2007**, *47*, 329–344.
8. Woodle, M. C. Controlling Liposome Blood Clearance by Surface-Grafted Polymers. *Adv. Drug Delivery Rev.* **1998**, *32*, 139–152.
9. Davis, M. E.; Chen, Z.; Shin, D. M. Nanoparticle Therapeutics: An Emerging Treatment Modality for Cancer. *Nat. Rev. Drug Discovery* **2008**, *7*, 771–782.
10. Castro, G. A.; Ferreira, L. A. M. Novel Vesicular and Particulate Drug Delivery Systems for Topical Treatment of Acne. *Expert Opin. Drug Delivery* **2008**, *5*, 665–679.
11. Sinico, C.; Fadda, A. M. Vesicular Carriers for Dermal Drug Delivery. *Expert Opin. Drug Delivery* **2009**, *6*, 813–825.
12. Zhang, L.; Granick, S. How To Stabilize Phospholipid Liposomes (Using Nanoparticles). *Nano Lett.* **2006**, *6*, 694–698.
13. Sekine, Y.; Moritani, Y.; Ikeda-Fukazawa, T.; Sasaki, Y.; Akiyoshi, K. A Hybrid Hydrogel Biomaterial by Nanogel Engineering: Bottom-Up Design with Nanogel and Liposome Building Blocks To Develop a Multidrug Delivery System. *Adv. Healthcare Mater.* **2012**, *1*, 722–728.
14. Michel, R.; Plostica, T.; Abezgauz, L.; Danino, D.; Gradzielski, M. Control of the Stability and Structure of Liposomes by Means of Nanoparticles. *Soft Matter* **2013**, *9*, 4167–4177.
15. Zhang, L.; Granick, S. Slaved Diffusion in Phospholipid Bilayers. *Proc. Natl. Acad. Sci. U. S. A.* **2005**, *102*, 9118–9121.

16. Wang, B.; Zhang, L.; Bae, S. C.; Granick, S. Nanoparticle-Induced Surface Reconstruction of Phospholipid Membranes. *Proc. Natl. Acad. Sci. U. S. A.* **2008**, *105*, 18171–18175.

17. Pornpattananangkul, D.; Olson, S.; Aryal, S.; Sartor, M.; Huang, C.-M.; Vecchio, K.; Zhang, L. Stimuli-Responsive Liposome Fusion Mediated by Gold Nanoparticles. *ACS Nano* **2010**, *4*, 1935–1942.

18. Thamphiwatana, S.; Fu, V.; Zhu, J.; Lu, D.; Gao, W.; Zhang, L. Nanoparticle-Stabilized Liposomes for pH-Responsive Gastric Drug Delivery. *Langmuir* **2013**, *29*, 12228–12233.

19. Pornpattananangkul, D.; Zhang, L.; Olson, S.; Aryal, S.; Obonyo, M.; Vecchio, K.; Huang, C.-M.; Zhang, L. Bacterial Toxin-Triggered Drug Release from Gold Nanoparticle-Stabilized Liposomes for the Treatment of Bacterial Infection. *J. Am. Chem. Soc.* **2011**, *133*, 4132–4139.

20. Suri, A.; Campos, R.; Rackus, D. G.; Spiller, N. J. S.; Richardson, C.; Palsson, L.-O.; Kataky, R. Liposome-Doped Hydrogel for Implantable Tissue. *Soft Matter* **2011**, *7*, 7071–7077.

21. Liu, Y.; Li, Z.; Liang, D. Behaviors of Liposomes in a Thermo-Responsive Poly(N-isopropylacrylamide) Hydrogel. *Soft Matter* **2012**, *8*, 4517–4523.

22. Peppas, N. A.; Hilt, J. Z.; Khademhosseini, A.; Langer, R. Hydrogels in Biology and Medicine: From Molecular Principles to Bionanotechnology. *Adv. Mater.* **2006**, *18*, 1345–1360.

23. Slaughter, B. V.; Khurshid, S. S.; Fisher, O. Z.; Khademhosseini, A.; Peppas, N. A. Hydrogels in Regenerative Medicine. *Adv. Mater.* **2009**, *21*, 3307–3329.

24. Hoffman, A. S. Hydrogels for Biomedical Applications. *Adv. Drug Delivery Rev.* **2012**, *64*, 18–23.

25. Liu, Y.; Liang, D. Hydrogel Integrated with Liposome: A Two-Stage Drug Delivery System. *J. Controlled Release* **2011**, *152*, E63–E64.

26. Popescu, M.-T.; Mourtas, S.; Pampalakis, G.; Antimisiaris, S. G.; Tsitsilianis, C. pH-Responsive Hydrogel/Liposome Soft Nanocomposites for Tuning Drug Release. *Biomacromolecules* **2011**, *12*, 3023–3030.

27. Khademhosseini, A.; Langer, R. Microengineered Hydrogels for Tissue Engineering. *Biomaterials* **2007**, *28*, 5087–5092.

28. Lee, J.-H.; Oh, H.; Baxa, U.; Raghavan, S. R.; Blumenthal, R. Biopolymer-Connected Liposome Networks as Injectable Biomaterials Capable of Sustained Local Drug Delivery. *Biomacromolecules* **2012**, *13*, 3388–3394.

29. Brandl, F.; Kastner, F.; Gschwind, R. M.; Blunk, T.; Tessmar, J.; Goepferich, A. Hydrogel-Based Drug Delivery Systems: Comparison of Drug Diffusivity and Release Kinetics. *J. Controlled Release* **2010**, *142*, 221–228.

30. Qiu, Y.; Park, K. Environment-Sensitive Hydrogels for Drug Delivery. *Adv. Drug Delivery Rev.* **2012**, *64*, 49–60.

31. Wilson, A. N.; Guiseppi-Elie, A. Bioresponsive Hydrogels. *Adv. Healthcare Mater.* **2013**, *2*, 520–532.

32. Negredo, E.; Puig, J.; Aldea, D.; Medina, M.; Estany, C.; Perez-Alvarez, N.; Rodriguez-Fumaz, C.; Munoz-Moreno, J. A.; Higueras, C.; Gonzalez-Mestre, V.; Clotet, B. Four-Year Safety with Polyacrylamide Hydrogel To Correct Antiretroviral-Related Facial Lipoatrophy. *AIDS Res. Hum. Retroviruses* **2009**, *25*, 451–455.

33. Darnell, M. C.; Sun, J.-Y.; Mehta, M.; Johnson, C.; Arany, P. R.; Suo, Z.; Mooney, D. J. Performance and Biocompatibility of Extremely Tough Alginate/Polyacrylamide Hydrogels. *Biomaterials* **2013**, *34*, 8042–8048.

34. Schaefer-Korting, M.; Mehnert, W.; Korting, H.-C. Lipid Nanoparticles for Improved Topical Application of Drugs for Skin Diseases. *Adv. Drug Delivery Rev.* **2007**, *59*, 427–443.

35. Schmid-Wendtner, M. H.; Korting, H. C. The pH of the Skin Surface and Its Impact on the Barrier Function. *Skin Pharmacol. Physiol.* **2006**, *19*, 296–302.

36. Greenman, J. Follicular pH and the Development of Acne. *Int. J. Dermatol.* **1981**, *20*, 656–658.

37. Holland, D. B.; Cunliffe, W. J. Skin Surface and Open Comedone pH in Acne Patients. *Acta Derm. Venereol.* **1983**, *63*, 155–158.

38. Ritger, P. L.; Peppas, N. A. A Simple Equation for Description of Solute Release I. Fickian and Non-Fickian Release from Non-Swellable Devices in the Form of Slabs Spheres Cylinders or Discs. *J. Controlled Release* **1987**, *5*, 23–36.

39. Casault, S.; Slater, G. W. Systematic Characterization of Drug Release Profiles from Finite-Sized Hydrogels. *Physica A* **2008**, *387*, 5387–5402.

40. Ashley, G. W.; Henise, J.; Reid, R.; Santi, D. V. Hydrogel Drug Delivery System with Predictable and Tunable Drug Release and Degradation Rates. *Proc. Natl. Acad. Sci. U. S. A.* **2013**, *110*, 2318–2323.

41. Higuchi, T. Rate of Release of Medicaments from Ointment Bases Containing Drugs in Suspension. *J. Pharm. Sci.* **1961**, *50*, 874–875.

42. Siepmann, J.; Peppas, N. A. Higuchi Equation: Derivation, Applications, Use and Misuse. *Int. J. Pharm.* **2011**, *418*, 6–12.

43. Huang, C.-M.; Chen, C.-H.; Pornpattananangkul, D.; Zhang, L.; Chan, M.; Hsieh, M.-F.; Zhang, L. Eradication of Drug Resistant Staphylococcus Aureus by Liposomal Oleic Acids. *Biomaterials* **2011**, *32*, 214–221.

44. Aryal, S.; Remant, B. K. C.; Dharmaraj, N.; Bhattarai, N.; Kim, C. H.; Kim, H. Y. Spectroscopic Identification of S-Au Interaction in Cysteine Capped Gold Nanoparticles. *Spectrochim. Acta, Part A* **2006**, *63*, 160–163.

45. Mayer, L. D.; Hope, M. J.; Cullis, P. R. Vesicles of Variable Sizes Produced by a Rapid Extrusion Procedure. *Biochim. Biophys. Acta* **1986**, *858*, 161–168.